

This article was downloaded by:

On: 23 January 2011

Access details: *Access Details: Free Access*

Publisher *Taylor & Francis*

Informa Ltd Registered in England and Wales Registered Number: 1072954 Registered office: Mortimer House, 37-41 Mortimer Street, London W1T 3JH, UK



Journal of Coordination Chemistry

Publication details, including instructions for authors and subscription information:

<http://www.informaworld.com/smpp/title~content=t713455674>

Supramolecular networks constructed from mono- and bi-nuclear lanthanide complexes with 1,2-phenylenedioxydiacetic acid

Yong Jiang^a; Xiao-Shuo Wu^a; Xia Li^a; Jin-Hao Song^a; Ying-Quan Zou^b

^a Department of Chemistry, Capital Normal University, Beijing 100048, China ^b Department of Chemistry, Beijing Normal University, Beijing 100875, China

First published on: 11 August 2009

To cite this Article Jiang, Yong , Wu, Xiao-Shuo , Li, Xia , Song, Jin-Hao and Zou, Ying-Quan(2010) 'Supramolecular networks constructed from mono- and bi-nuclear lanthanide complexes with 1,2-phenylenedioxydiacetic acid', Journal of Coordination Chemistry, 63: 1, 36 – 45, First published on: 11 August 2009 (iFirst)

To link to this Article: DOI: 10.1080/00958970903186431

URL: <http://dx.doi.org/10.1080/00958970903186431>

PLEASE SCROLL DOWN FOR ARTICLE

Full terms and conditions of use: <http://www.informaworld.com/terms-and-conditions-of-access.pdf>

This article may be used for research, teaching and private study purposes. Any substantial or systematic reproduction, re-distribution, re-selling, loan or sub-licensing, systematic supply or distribution in any form to anyone is expressly forbidden.

The publisher does not give any warranty express or implied or make any representation that the contents will be complete or accurate or up to date. The accuracy of any instructions, formulae and drug doses should be independently verified with primary sources. The publisher shall not be liable for any loss, actions, claims, proceedings, demand or costs or damages whatsoever or howsoever caused arising directly or indirectly in connection with or arising out of the use of this material.

Supramolecular networks constructed from mono- and bi-nuclear lanthanide complexes with 1,2-phenylenedioxydiacetic acid

YONG JIANG[†], XIAO-SHUO WU[†], XIA LI*[†], JIN-HAO SONG[†]
and YING-QUAN ZOU[‡]

[†]Department of Chemistry, Capital Normal University, Beijing 100048, China

[‡]Department of Chemistry, Beijing Normal University, Beijing 100875, China

(Received 11 April 2009; in final form 7 June 2009)

[Tb₂(1,2-pdoa)₃·6H₂O]·H₂O (**1**) and [La(1,2-pdoa)(1,2-H₂pdoa)(OH)·H₂O]·5H₂O (**2**) (1,2-H₂pdoa = 1,2-phenylenedioxydiacetic acid) have been synthesized and structurally characterized by single crystal X-ray diffraction. Complex **1** is a binuclear molecule in which one 1,2-pdoa ligand is a tetradentate bridge linking two Tb³⁺ ions, the other two 1,2-pdoa ligands bond Tb1³⁺ and Tb1A³⁺ via tetradentate chelating coordination. Tb³⁺ is nine-coordinate by six oxygens of 1,2-pdoa and three waters. Complex **2** is mono-nuclear with La³⁺ ten-coordinate by eight oxygens of two 1,2-pdoa, one hydroxide and one water. 1,2-Pdoa is tetradentate chelating with La³⁺ ion. The packing diagrams of **1** and **2** show supramolecular networks via H-bonds. The fluorescence spectrum of **1** shows characteristic emission of Tb³⁺ with ⁵D₄ → ⁷F_j (j = 6–3) transitions.

Keywords: Lanthanide complex; 1,2-Phenylenedioxydiacetic acid; Crystal structure; Fluorescence

1. Introduction

Inorganic–organic complexes have received remarkable attention due to their intriguing architectures and potential applications in catalysis, absorption, fluorescent materials, etc. [1–10]. Lanthanide(III) ions have unique spectroscopic and magnetic properties. Lanthanide carboxylate complexes have various structures resulting from coordination versatility of carboxylate and such compounds often have intense luminescence and high thermal stability. In particular, polycarboxylate ligands have been extensively used for construction of metal complexes by chelating and bridging coordination modes, forming polymeric or network structures. Lanthanide complexes with 1-D, 2-D, and 3-D structures based on polycarboxylic acid have been reported [8–14]. Discrete mono- and bi-nuclear molecules are less reported [15–18]. However, noncovalent interactions such as H-bonds and π – π stacking in crystal lattice can lead to higher-dimensionality supramolecular structures from discrete molecular

*Corresponding author. Email: Xiali@mail.cnu.edu.cn

building blocks. The phenylenedioxydiacetates (pdoa) are multidentate ligands through the four carboxylate oxygen and two ether oxygens linking metal ions. Some lanthanide complexes with pdoa have been synthesized and structurally characterized [11–14] with polymeric structures, in which metal ions are linked by the metal-ligand coordination bonds. Only a few lanthanide complexes with 1,2-pdoa have been reported [16]. We obtained $[\text{Tb}_2(1,2\text{-pdoa})_3 \cdot 6\text{H}_2\text{O}] \cdot \text{H}_2\text{O}$ (**1**) and $[\text{La}(1,2\text{-pdoa})(1,2\text{-H}_2\text{pdoa})(\text{OH}) \cdot \text{H}_2\text{O}] \cdot 5\text{H}_2\text{O}$ (**2**) (1,2-H₂pdoa = 1,2-phenylenedioxydiacetic acid) with bi-nuclear and mono-nuclear structures, respectively, and supramolecular structures are formed by H-bonds. The two complexes are different from other metal-carboxylate complexes, which show 1-D, 2-D or 3-D polymeric structures by covalent bands [19–24]. In this article, the syntheses and structural characteristics of the two complexes are reported. The present structures differ from those reported for lanthanide complexes based on mono- or poly-carboxylates.

2. Experimental

2.1. Materials

$\text{Ln}(\text{NO}_3)_3 \cdot 6\text{H}_2\text{O}$ was prepared from the corresponding oxide with nitric acid. Other analytical grade chemicals and solvents were purchased and used without purification.

2.2. Synthesis of the complexes

1,2-Phenylenedioxydiacetic acid (0.15 mmol) was dissolved in 15 mL ethanol and the pH adjusted to 5–6 by 2 mol L^{-1} aqueous NaOH. Then 5 mL ethanol solution of 0.1 mmol $\text{Ln}(\text{NO}_3)_3 \cdot 6\text{H}_2\text{O}$ (Ln = Tb and La) was added to the solution, and the mixture was refluxed with stirring for 1 h. The resulting solution was filtered and after several days colorless single crystals were deposited from the filtrate. Yield, about 46%. For **1**, $\text{C}_{30}\text{H}_{40}\text{O}_{26}\text{Tb}_2$ (1134.46), Calcd: C, 31.73; H, 3.52. Found: C, 31.58; H, 3.39%. Selected IR (KBr pellet, $\nu \text{ cm}^{-1}$): 3169 br, 1623 vs, 1504 s, 1437 s, 1256 s, 1127 s, 964 w, 753 m, 618 w, 462 w. For **2**, $\text{C}_{20}\text{H}_{31}\text{LaO}_{19}$ (714.36), Calcd: C, 33.63; H, 4.37. Found: C, 33.48; H, 4.22%. Selected IR (KBr pellet, $\nu \text{ cm}^{-1}$): 3443 br, 1616 vs, 1505 s, 1423 s, 1250 s, 1125 s, 950 m, 823 m, 684 w, 524 w.

2.3. Single-crystal X-ray diffraction

The X-ray single crystal data collections for both complexes were performed on a Bruker Smart Apex II CCD diffractometer equipped with graphite monochromated Mo-K α radiation ($\lambda = 0.71073 \text{ \AA}$) at 293(2) K. Semiempirical absorption corrections were applied. The structures were solved by direct methods and refined by full-matrix least-squares on F^2 using the SHELXTL-97 software package [25, 26]. All non-hydrogen atoms in the two complexes were refined anisotropically. The hydrogens were generated geometrically and treated by a mixture of independent and constrained refinement. The summary of crystal data and selected bond lengths and angles for **1** and **2** are listed in tables 1–3.

Table 1. Crystal data and structure refinement for **1** and **2**.

Complex	1	2
Empirical formula	C ₃₀ H ₄₀ O ₂₆ Tb ₂	C ₂₀ H ₃₁ LaO ₁₉
Formula weight	1134.46	714.37
Temperature (K)	293(2)	296(2)
Crystal system	Orthorhombic	Triclinic
Space group	<i>Pbca</i>	<i>P</i> $\bar{1}$
Unit cell dimensions (Å, °)		
<i>a</i>	16.6402(16)	8.7895(4)
<i>b</i>	8.0058(8)	12.3613(5)
<i>c</i>	30.999(3)	12.7552(5)
α	90	75.899(2)
β	90	78.542(2)
γ	90	84.790(2)
Volume (Å ³), <i>Z</i>	4129.6(7), 4	1315.99(10), 1
Calculated density (mg m ⁻³)	1.825	1.798
Absorption coefficient (mm ⁻¹)	3.488	1.712
<i>F</i> (000)	2232	716
Crystal size (mm ³)	0.30 × 0.15 × 0.07	0.30 × 0.15 × 0.10
θ range for data collection (°)	2.45–27.90	1.70–25.01
Limiting indices	−16 ≤ <i>h</i> ≤ 21; −10 ≤ <i>k</i> ≤ 10; −39 ≤ <i>l</i> ≤ 29	−10 ≤ <i>h</i> ≤ 10; −14 ≤ <i>k</i> ≤ 14; −15 ≤ <i>l</i> ≤ 15
Reflections collected	18,648	11,182
Independent reflection	4891 [<i>R</i> _{int} = 0.0227]	4440 [<i>R</i> _{int} = 0.0185]
Data/restraints/parameters	4891/18/281	4440/0/380
Goodness-of-fit on <i>F</i> ²	1.170	1.556
Final <i>R</i> indices [<i>I</i> > 2σ(<i>I</i>)]	<i>R</i> ₁ = 0.0412, <i>wR</i> ₂ = 0.1059	<i>R</i> ₁ = 0.0326, <i>wR</i> ₂ = 0.0897
<i>R</i> indices (all data)	<i>R</i> ₁ = 0.0498, <i>wR</i> ₂ = 0.1094	<i>R</i> ₁ = 0.0350, <i>wR</i> ₂ = 0.0962
Largest difference peak and hole (e Å ⁻³)	1.489 and −1.880	2.093 and −0.727

Table 2. Bond lengths (Å) and angles (°) for **1**.

Tb(1)–O(5)	2.319(4)	Tb(1)–O(8)	2.409(5)
Tb(1)–O(7)	2.506(4)	Tb(1)–O(1)	2.358(4)
Tb(1)–O(3)	2.529(4)	Tb(1)–O(12)	2.386(4)
Tb(1)–O(4)	2.582(4)	Tb(1)–O(10)	2.393(4)
		Tb(1)–O(11)	2.407(4)
O(5)–Tb(1)–O(1)	153.96(17)	O(11)–Tb(1)–O(7)	131.19(15)
O(5)–Tb(1)–O(12)	88.65(16)	O(8)–Tb(1)–O(7)	52.66(14)
O(1)–Tb(1)–O(12)	97.13(16)	O(5)–Tb(1)–O(3)	123.28(14)
O(5)–Tb(1)–O(10)	83.93(18)	O(1)–Tb(1)–O(3)	64.65(12)
O(1)–Tb(1)–O(10)	75.45(17)	O(12)–Tb(1)–O(3)	141.06(14)
O(12)–Tb(1)–O(10)	140.48(16)	O(10)–Tb(1)–O(3)	71.09(14)
O(5)–Tb(1)–O(11)	77.12(17)	O(11)–Tb(1)–O(3)	133.27(15)
O(1)–Tb(1)–O(11)	81.00(15)	O(8)–Tb(1)–O(3)	86.11(16)
O(12)–Tb(1)–O(11)	70.26(16)	O(7)–Tb(1)–O(3)	69.01(14)
O(10)–Tb(1)–O(11)	70.24(15)	O(5)–Tb(1)–O(4)	63.92(14)
O(5)–Tb(1)–O(8)	81.10(17)	O(1)–Tb(1)–O(4)	121.80(13)
O(1)–Tb(1)–O(8)	124.95(15)	O(12)–Tb(1)–O(4)	137.88(16)
O(12)–Tb(1)–O(8)	76.85(18)	O(10)–Tb(1)–O(4)	71.18(16)
O(10)–Tb(1)–O(8)	139.25(17)	O(11)–Tb(1)–O(4)	127.00(14)
O(11)–Tb(1)–O(8)	140.60(18)	O(8)–Tb(1)–O(4)	68.18(15)
O(5)–Tb(1)–O(7)	132.62(16)	O(7)–Tb(1)–O(4)	101.80(14)
O(1)–Tb(1)–O(7)	73.04(14)	O(3)–Tb(1)–O(4)	60.02(12)
O(12)–Tb(1)–O(7)	72.84(15)	O(10)–Tb(1)–O(7)	136.77(15)

Table 3. Bond lengths (Å) and angles (°) for **2**.

La(1)–O(11)	2.489(3)	La(1)–O(8)	2.494(3)
La(1)–O(25)	2.502(3)	La(1)–O(6)	2.506(3)
La(1)–O(3)	2.528(3)	La(1)–O(5W)	2.621(3)
La(1)–O(10)	2.644(3)	La(1)–O(4)	2.709(3)
La(1)–O(9)	2.712(3)	La(1)–O(1)	2.739(3)
O(11)–La(1)–O(8)	137.66(10)	O(11)–La(1)–O(25)	137.58(11)
O(8)–La(1)–O(25)	73.31(11)	O(11)–La(1)–O(6)	116.83(10)
O(8)–La(1)–O(6)	98.12(10)	O(25)–La(1)–O(6)	72.54(11)
O(11)–La(1)–O(3)	88.33(10)	O(8)–La(1)–O(3)	71.52(10)
O(25)–La(1)–O(3)	74.63(11)	O(6)–La(1)–O(3)	147.16(10)
O(11)–La(1)–O(5W)	66.22(10)	O(8)–La(1)–O(5W)	72.38(10)
O(25)–La(1)–O(5W)	138.87(10)	O(6)–La(1)–O(5W)	134.35(10)
O(3)–La(1)–O(5W)	73.52(10)	O(11)–La(1)–O(10)	61.44(9)
O(8)–La(1)–O(10)	114.79(10)	O(8)–La(1)–O(10)	114.79(10)
O(6)–La(1)–O(10)	70.68(10)	O(25)–La(1)–O(10)	143.09(11)
O(5W)–La(1)–O(10)	73.52(10)	O(3)–La(1)–O(10)	142.14(10)
O(8)–La(1)–O(4)	151.50(11)	O(11)–La(1)–O(4)	70.83(10)
O(6)–La(1)–O(4)	59.41(10)	O(25)–La(1)–O(4)	82.60(11)
O(3)–La(1)–O(4)	116.84(10)	O(3)–La(1)–O(4)	116.84(10)
O(10)–La(1)–O(4)	76.37(10)	O(5W)–La(1)–O(4)	135.50(10)
O(11)–La(1)–O(9)	112.77(10)	O(11)–La(1)–O(9)	112.77(10)
O(25)–La(1)–O(9)	108.64(11)	O(8)–La(1)–O(9)	59.18(9)
O(3)–La(1)–O(9)	125.75(9)	O(6)–La(1)–O(9)	65.95(10)
O(10)–La(1)–O(9)	57.89(9)	O(5W)–La(1)–O(9)	71.39(10)
O(11)–La(1)–O(1)	66.67(10)	O(4)–La(1)–O(9)	117.26(10)
O(8)–La(1)–O(1)	125.32(9)	O(25)–La(1)–O(1)	71.20(11)
O(6)–La(1)–O(1)	109.00(10)	O(3)–La(1)–O(1)	59.85(9)
O(3)–La(1)–O(1)	59.85(9)	O(5W)–La(1)–O(1)	112.63(10)
O(10)–La(1)–O(1)	118.70(9)	O(9)–La(1)–O(1)	174.34(9)
O(4)–La(1)–O(1)	57.10(9)		

2.4. Physical measurement

Elemental analyses (C, H, N) were performed using an Elementar Vario EL analyzer. IR spectra were recorded with a Bruker EQUINOX-55 spectrometer using KBr pellets from 400 to 4000 cm^{-1} . Thermogravimetric analyses were carried out on a WCT-1A Thermal Analyzer at a heating rate of 10 $^{\circ}\text{C min}^{-1}$ from 20 $^{\circ}\text{C}$ to 1000 $^{\circ}\text{C}$ in air. Excitation and emission spectra of the solid sample were recorded on an F-4500 Fluorescence Spectrophotometer at room temperature.

3. Results and discussion

3.1. Structural description of $[\text{Tb}_2(1,2\text{-pdoa})_3 \cdot 6\text{H}_2\text{O}] \cdot \text{H}_2\text{O}$ (**1**)

The crystal structure of **1** is shown in figure 1. **1** consists of a dimeric unit $[\text{Tb}_2(1,2\text{-pdoa})_3 \cdot 6\text{H}_2\text{O}]$ (figure 1a) and a free water. 1,2-pdoa coordinate Tb^{3+} by tetradentate-bridging and tetradentate-chelating. Two Tb^{3+} ions are linked through a single tetradentate-bridging 1,2-pdoa via its two bidentate-chelating carboxylates to form a centrosymmetric dimeric unit. Each Tb^{3+} is also chelated by one tetradentate-chelating 1,2-pdoa through its two monodentate carboxylates and two ether oxygens, forming three, five-membered chelating rings. Three waters complete the distorted monocapped square antiprism of Tb^{3+} . O1, O3, O8, O12, and O4, O5, O10, O11 form the upper and lower square planes with mean deviations of 0.1247 and 0.3157 Å, respectively.

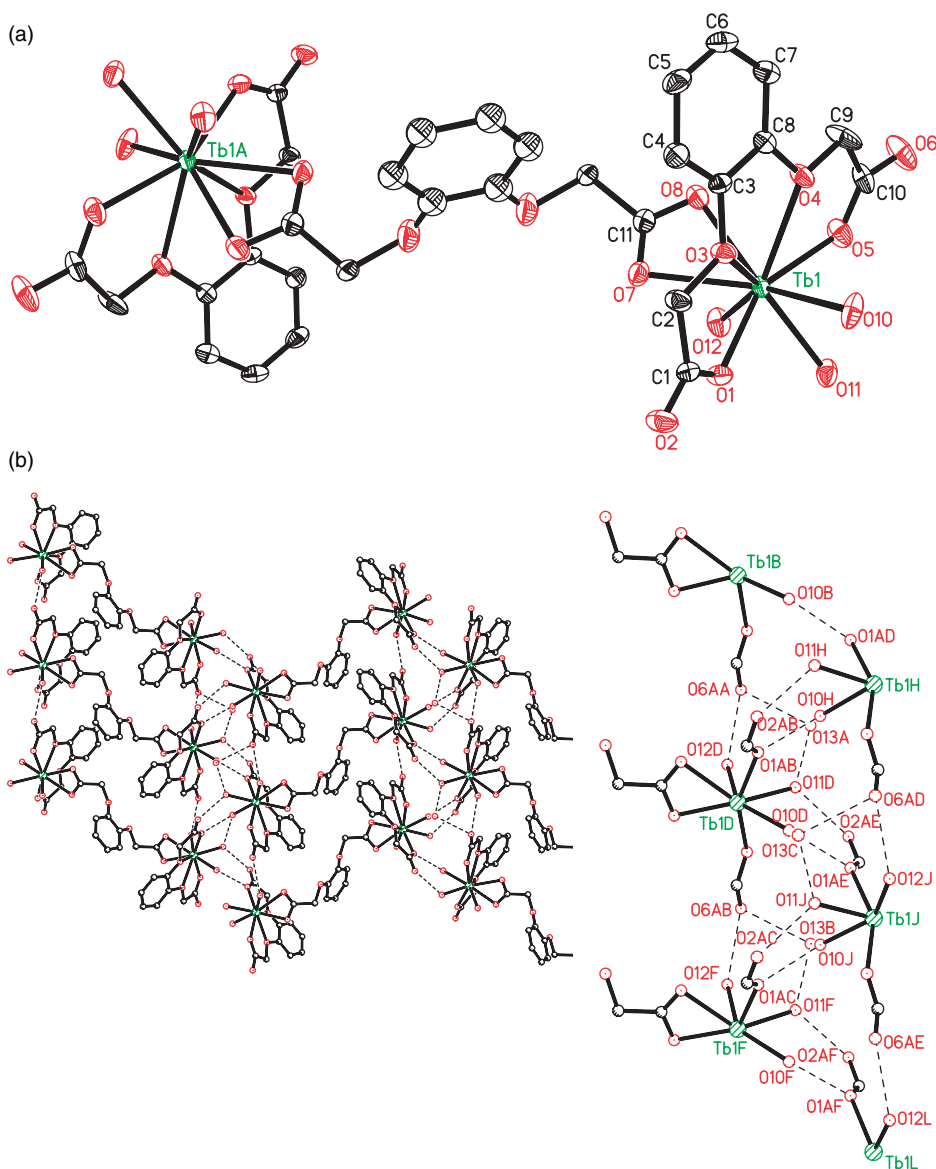


Figure 1. (a) Molecular structure of **1** with 30% probability displacement ellipsoids. Free water and all hydrogen atoms are omitted for clarity. (b) Packing diagram of **1** showing 2-D network and H-bonds along the *a*-axis.

The dihedral angle between them is 4.7° . O7 caps the monocapped square antiprism. The average distances of Tb–O(carboxylate), Tb–O(ether) and Tb–O(water) are 2.398, 2.556, and 2.395 Å, respectively. The O–Tb–O bond angles range from $52.66(14)^\circ$ to $153.96(17)^\circ$.

This binuclear structure is different from the structures of many other dimeric lanthanide carboxylate complexes, such as $[\text{Tb}(2\text{-FBA})_3 \cdot (2\text{-HFBA}) \cdot \text{H}_2\text{O}]_2$ (2-HFBA = 2-fluorobenzoic acid) [27] and $[\text{Tb}_2(\text{Hsal})_8(\text{H}_2\text{O})_2][(\text{Hphen})_2] \cdot 2\text{H}_2\text{O}$

(Hsal = *o*-HOC₆H₄CO₂, phen = 1,10-phenanthroline) [28], where two Tb³⁺ ions are separated by two, three, or four COO⁻ groups via bidentate-bridging and/or tridentate bridging-chelating coordination. In **1** Tb³⁺ ions are separated by a long and single 1,2-pdoa anion as bridge. In **1** the Tb1...Tb1A distance of 12.420 Å is much longer than Tb...Tb distances in other reported terbium(III) dimers containing carboxylates [27–29].

Coordinated waters (O10 and O11) form H-bonds with uncoordinated carboxylate (O2) and coordinated carboxylate (O1) from adjacent molecules form a 1-D chain along the *b*-axis, O10–H2W...O1 [–*x*, *y* + ½, –*z* + ½], 2.733 Å, 171.88° and O11–H4W...O2 [–*x*, *y* + ½, –*z* + ½], 2.708 Å, 175.75°. The coordinated waters (O12) form H-bonds with uncoordinated carboxylate (O6) from adjacent molecules to form a 1-D chain along the *c*-axis, O12–H5W...O6 [–*x* – ½, *y* – ½, *z*], 2.769 Å, 160.84°; O12–H6W...O6 [*x*, *y* – 1, *z*], 2.815 Å, 177.83°. Such strong H-bonds connect the discrete binuclear molecules along *b*- and *c*-axes, generating a 2-D network as shown in figure 1(b). Furthermore, the free water (O13) is involved in H-bonds with coordinated waters (O10 and O11), O10–H1W...O13 [–*x*, *y* + ½, –*z* + ½] 2.995 Å, 168.46°; and O11–H3W...O13, 2.733 Å, 169.78°, further connecting the discrete molecules in 2-D sheets.

3.2. Structural description of [La(1,2-pdoa)(1,2-H₂pdoa)(OH)H₂O] · 5H₂O (**2**)

Complex **2** crystallizes in the triclinic crystal system with *P*₁ space group, different from **1** (*Pbca* space group). Complex **2** consists of [La(1,2-pdoa)(1,2-H₂pdoa)(OH)H₂O] [figure 2(a)] and five free water molecules. La³⁺ is chelated by 1,2-pdoa and 1,2-H₂pdoa, forming six, five-membered chelation rings. Complex **2** contains two different 1,2-H₂pdoa motifs, one completely deprotonated coordinating La³⁺ using two carboxylate oxygens and two ether oxygens; the other 1,2-H₂pdoa is not deprotonated coordinating La³⁺ using two carboxylate hydroxyl and two ether oxygens. The La³⁺ is further coordinated by water and hydroxide to complete ten-coordination. The LaO₁₀ can be described as a distorted bicapped square antiprism, in which the upper and lower square planes are defined by O3, O4, O11, O25 and O5W, O6, O8, O10, respectively, with mean deviations of 0.2382 and 0.2105 Å. The dihedral angle between the two planes is 2.1°. O1 and O9 cap the upper and lower planes, respectively. The average distances of La–O(carboxylate), La–O(ether), La–O(hydroxyl), and La–O(water) are 2.504, 2.701, 2.502, and 2.621 Å, respectively, with the O–La–O bond angles ranging from 57.10(9)° to 174.34(9)°.

Free waters (O1W, O2W, O3W, O4W, and O6W) are present within the crystal and participate in H-bonds. The coordinated water (O5W), uncoordinated carboxylates (O5 and O7), coordinated carboxylates (O3, O6, and O11), and hydroxide (O25) also participate in H-bond formation. Multiple H-bond interactions result in formation of a 3-D H-bond network [figure 2(b)]. Hydrogen bond distances are in the range 2.543–2.900 Å and O...H–O angles are in the range of 113.19°–173.45° (Supplementary material). Discrete mono-nuclear units are connected through strong 3-D H-bond network, yielding a 3-D supramolecular structure, illustrated in figure 2(b).

The structures of **1** and **2** are different from many other lanthanide complexes based on polycarboxylate. A large number of lanthanide polycarboxylate complexes show 1-D, 2-D, or 3-D polymeric structures [8–14] and a few are discrete molecules [15–18].

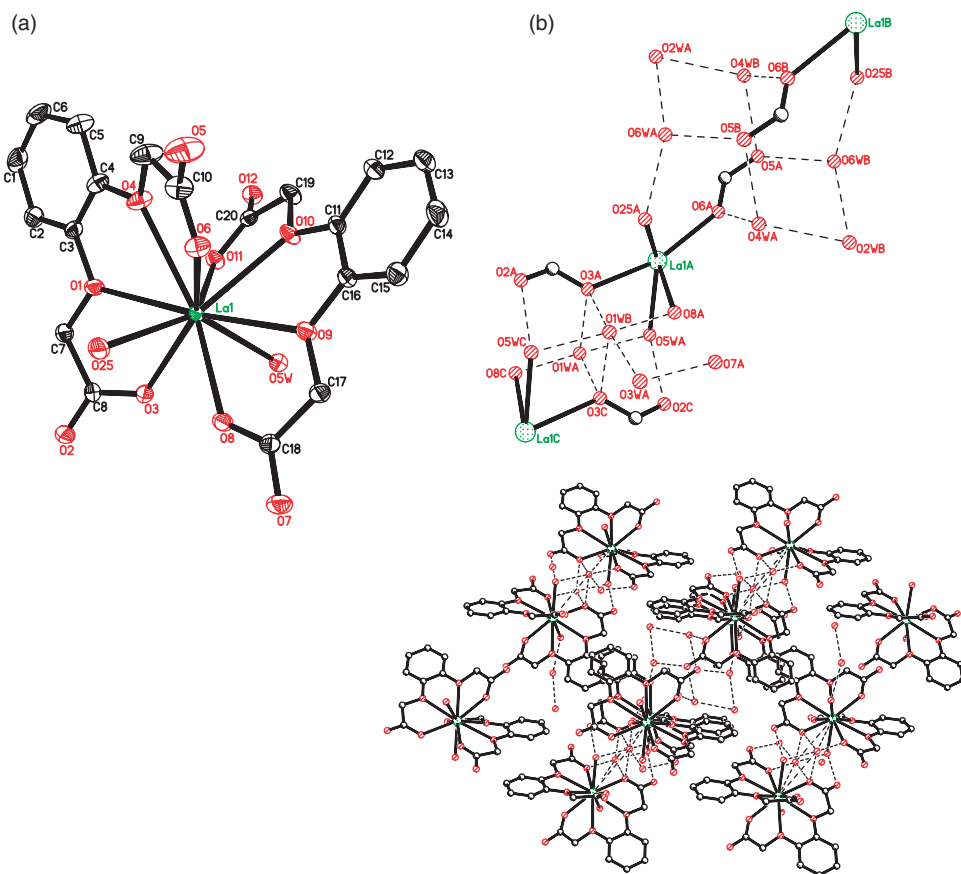


Figure 2. (a) Molecular structure of **2** at 30% probability displacement ellipsoids. Free water and all hydrogens are omitted for clarity. (b) Packing diagram of **2** showing 3-D network and H-bonds along the *a*-axis.

Comparison of **2** with **1** shows that the corresponding distances decrease, namely $d(\text{La}-\text{O}(\text{carboxylate})) > d(\text{Tb}-\text{O}(\text{carboxylate}))$, $d(\text{La}-\text{O}(\text{ether})) > d(\text{Tb}-\text{O}(\text{ether}))$ and $d(\text{La}-\text{O}(\text{water})) > d(\text{Tb}-\text{O}(\text{water}))$, caused by the decrease in ion radii from the La^{3+} to Tb^{3+} ions. The coordination number of La^{3+} ion in **2** is more than that of Tb^{3+} ion in **1**, also in agreement with the greater La^{3+} ion radius. These differences are in accord with the effect of the lanthanide contraction.

3.3. Thermogravimetric analysis

The thermal behavior of the two complexes was studied from 20°C to 1000°C. For **1**, the first weight loss occurs between 126–171°C, from loss of all water molecules. The observed weight loss of 12.76% is close to the calculated value of 12.69%. After loss of water, there is no other weight loss before 341°C, when organic ligands decompose leaving Tb_4O_7 (Obs: 68.15%, Calcd 67.70%). For **2**, the first weight loss occurs from 107–151°C, assigned to loss of all water (Obs: 12.61%, Calcd 13.51%).

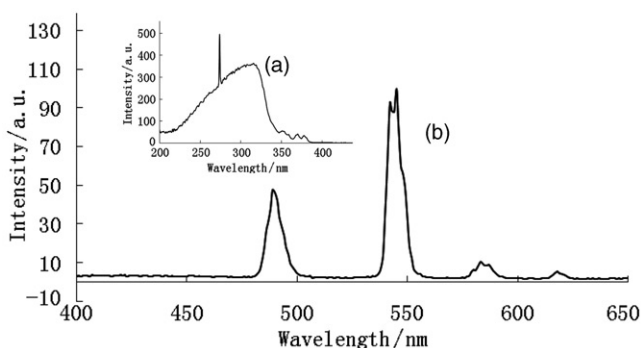


Figure 3. Luminescence spectra for **1**: (a) Excitation ($\lambda_{em} = 545$ nm); (b) Emission ($\lambda_{ex} = 351$ nm).

Decomposition of organic ligand starts at 381°C . The final residue is $\text{La}_2\text{O}_2\text{CO}_3$ (Obs: 69.52%, Calcd 73.91%) [30–32].

3.4. Luminescence properties for (**1**)

Complex **1** emits bright green light in the solid state under UV irradiation. The excitation and emission spectra of the solid sample were recorded on an F-4500 Fluorescence Spectrophotometer at room temperature (figure 3). The excitation spectrum of **1** under the intense $^5\text{D}_4 \rightarrow ^7\text{F}_5$ transition (545 nm) of Tb^{3+} ion is composed of a wide band and narrow bands. A wide excitation band between 200 and 340 nm corresponds to $\pi-\pi^*$ transition of the ligand. Narrow excitation bands arise from Tb^{3+} intra- $4f^8$ at 351 ($^5\text{G}_2$), 371 ($^5\text{D}_2$) and 379 ($^5\text{D}_3$) nm [33]. The relatively high intensities of the ligand indicate that the Tb^{3+} ion is excited by ligand triplet states and direct excitation into the emissive states. Narrow emission bands are observed upon excitation at 351 nm corresponding to the characteristic f–f transitions of Tb^{3+} . The strongest emission at 545 nm with a shoulder of 542 nm corresponds to $^5\text{D}_4 \rightarrow ^7\text{F}_5$. The second largest peak at 489 nm corresponds to the $^5\text{D}_4 \rightarrow ^7\text{F}_6$ transition. The weak peaks at 583 nm with a shoulder of 590 nm and 618 nm correspond to the $^5\text{D}_4 \rightarrow ^7\text{F}_4$ and $^5\text{D}_4 \rightarrow ^7\text{F}_3$ transitions, respectively. $\text{Tb}(\text{NO}_3)_3 \cdot 6\text{H}_2\text{O}$ (Tb^{3+}) has weak luminescence. However, Tb-coordination compounds have intense luminescence because emission of Tb^{3+} ion in its coordination compounds is caused by intramolecular energy transfer that consists of energy absorption by organic ligands, intersystem crossing into a triplet state of the organic ligands, and energy transfer to the Tb^{3+} , showing the ligand can sensitize luminescence of Tb^{3+} .

4. Conclusions

We obtained Tb(III) and La(III) complexes **1** and **2** using 1,2-phenylenedioxydiacetic acid. The different coordination modes of 1,2-pdoa ligands lead to **1** and **2** being dinuclear and mononuclear, respectively. The structures of **1** and **2** represent rarely reported discrete complexes based on polycarboxylic acid. A feature of the two

complexes is that the discrete structures are further connected to supramolecular networks by intramolecular H-bonds.

Supplementary material

CCDC-699806 for **1** and 715144 for **2** contain the supplementary crystallographic data for this article. These data can be obtained free of charge from CCDC, 12 Union Road, Cambridge, CB2 1EZ, UK (Fax: +44(0)1223-336033; E-mail: deposit@ccdc.cam.ac.uk).

Acknowledgment

We are grateful to the Science and Technology Program, Beijing Municipal Education Commission (KM200910028010).

References

- [1] S.L. James. *Chem. Soc. Rev.*, **32**, 276 (2003).
- [2] U. Mueller, M. Schubert, F. Teich, H. Putter, K. Schierle-Arndt, J. Pastre. *J. Mater. Chem.*, **16**, 626 (2006).
- [3] A.G. Wong-Foy, A.J. Matzger, O.M. Yaghi. *J. Am. Chem. Soc.*, **128**, 3494 (2006).
- [4] N.E. Chakov, S.C. Lee, A.G. Harter, P.L. Kuhns, A.P. Reyes, S.O. Hill, N.S. Dalal, W. Wernsdorfer, K.A. Abboud, G. Christou. *J. Am. Chem. Soc.*, **128**, 6975 (2006).
- [5] C. Janiak. *Dalton Trans.*, **14**, 2781 (2003).
- [6] M.B. Salah, S. Vilminot, G. Andre, M. Richard-Plouet, T. Mhiri, S. Takagi, M. Kurmoo. *J. Am. Chem. Soc.*, **128**, 7972 (2006).
- [7] D. Maspoch, D. Ruiz-Molina, J. Vecina. *J. Mater. Chem.*, **14**, 2713 (2004).
- [8] S.K. Ghosh, J.P. Zhang, S. Kitagawa. *Angew. Chem.*, **46**, 7965 (2007).
- [9] J.W. Ye, J. Wang, J.Y. Zhang, P. Zhang, Y. Wang. *CrystEngComm.*, **9**, 515 (2007).
- [10] C.A. Black, J.S. Costa, W.T. Fu, C. Massera, O. Roubeau, S.J. Teat, G. Aroml, P. Gamez, J. Reedijk. *Inorg. Chem.*, **48**, 1062 (2009).
- [11] X.F. Li, Z.B. Han, X.N. Cheng, X.M. Chen. *Inorg. Chem. Commun.*, **9**, 1091 (2006).
- [12] X.L. Hong, Y.Z. Li, H.M. Hu, Y. Pan, J.F. Bai, X.Z. You. *Cryst. Growth Des.*, **6**, 1221 (2006).
- [13] X. Li, Y.Q. Li, Y.B. Zhang. *J. Coord. Chem.*, **61**, 1720 (2008).
- [14] Y.C. Qiu, C. Daigebonne, J.Q. Liu, R.H. Zeng, N. Kerbellec, H. Deng, O. Guillou. *Inorg. Chim. Acta*, **360**, 3265 (2007).
- [15] B. Barja, R. Baggio, M.T. Garland, P.F. Aramendia, O. Pen, M. Perec. *Inorg. Chim. Acta*, **346**, 187 (2003).
- [16] X. Li, Y.Q. Li, X.J. Zheng, H.L. Sun. *Inorg. Chem. Commun.*, **11**, 779 (2008).
- [17] B. Yan, Y.S. Song, Z.X. Chen. *J. Mol. Struct.*, **694**, 115 (2004).
- [18] M. Liang, Y.Q. Sun, D.Z. Liao, Z.H. Jiang, S.P. Yan, P. Cheng. *J. Coord. Chem.*, **57**, 275 (2004).
- [19] W. Starosta, J. Leciejewicz. *J. Coord. Chem.*, **62**, 1240 (2009).
- [20] Y.F. Deng, Z.H. Zhou. *J. Coord. Chem.*, **62**, 1484 (2009).
- [21] A. Ramazani, L. Dolatyari, A. Morsali, M.Z. Kassae. *J. Coord. Chem.*, **62**, 1784 (2009).
- [22] P.P. Long, Q. Zhao, J.X. Dong, J.P. Li. *J. Coord. Chem.*, **62**, 1959 (2009).
- [23] Z.Q. Ming, Y.X. Miao, S.F. Si. *J. Coord. Chem.*, **62**, 833 (2009).
- [24] Y.H. Wen, X.H. Wu, S. Bi, S.S. Zhang. *J. Coord. Chem.*, **62**, 1249 (2009).
- [25] G.M. Sheldrick. *Acta Cryst.*, **A46**, 67 (1990).
- [26] G.M. Sheldrick. *SHELXL97, Program for X-ray Crystal Structure Solution*, University of Göttingen, Germany (1997).

- [27] X. Li, Z.Y. Zhang, Y.Q. Zou. *Eur. J. Inorg. Chem.*, 2909 (2005).
- [28] M.C. Yin, C.C. Ai, L.J. Yuan, C.W. Wang, J.T. Sun. *J. Mol. Struct.*, **691**, 33 (2004).
- [29] X. Li, Y.L. Ju, Y.Q. Li. *J. Coord. Chem.*, **61**, 692 (2008).
- [30] F. Wiesława, W.D. Agnieszka. *J. Serb. Chem. Soc.*, **66**, 543 (2001).
- [31] W. Brzyska, A. Kula. *J. Therm. Anal. Calorim.*, **53**, 161 (1998).
- [32] A. Kula. *J. Therm. Anal. Calorim.*, **75**, 79 (2004).
- [33] P.I. Girginova, F.A.A. Paz, P.C.R. Soares-Santos, R.A.S. Ferreira, L.D. Carlos, V.S. Amaral, J. Klinowski, H.I.S. Nogueira, T. Trindade. *Eur. J. Inorg. Chem.*, 4238 (2007).